ELSEVIER

Journal of Chromatography A, 811 (1998) 35–45

JOURNAL OF CHROMATOGRAPHY A

Forward-scattering degenerate four-wave mixing for sensitive absorption detection in microseparation systems Coupling to micro-column liquid chromatography

Tjipke de Beer, Gerard Ph. Hoornweg, Arjan Termaten, Udo A.Th. Brinkman, Nel H. Velthorst, Cees Gooijer*

Department of General and Analytical Chemistry, Free University, De Boelelaan 1083, 1081 HV Amsterdam, The Netherlands

Received 26 January 1998; received in revised form 27 March 1998; accepted 27 March 1998

Abstract

The feasibility of forward-scattering degenerate four-wave mixing (F-D4WM) for detection in micro-column (internal diameter 0.3 mm) liquid chromatography (micro-LC) is studied, using the separation of 1-amino-9,10-anthraquinone (I-AAQ) and 2-amino-9,10-anthraquinone (II-AAQ) as a model system and utilizing the 514 nm line of an argon-ion laser. Though the F-D4WM signal can be detected on a virtually dark background, in practice background reduction is of utmost importance. Background reduction by means of a mechanical chopper and a scanning confocal Fabry–Perot interferometer (CFP) are compared both experimentally and theoretically. Using the CFP set-up, an injected concentration limit of detection of $3 \cdot 10^{-8}$ *M* could be achieved for I-AAQ (molar absorptivity of $2 \cdot 10^{3}$ M^{-1} cm^{-1} at 514 nm), which is roughly two decades more favourable than obtained when using the mechanical chopper. In comparison to conventional absorption detection in micro-LC at 514 nm, the gain is also about two decades. In view of the fact that the present F-D4WM set-up still suffers from significant band broadening caused by the detector cell, further improvement seems possible.

Keywords: Four-wave mixing; Detection, LC; Absorbance detection; Interferometry; Instrumentation; Micro-LC; Amino-anthraquinones

1. Introduction

A major trend in analytical chemistry is miniaturization of liquid separation systems to achieve extremely high separation power; this has led to a growing interest in microseparation systems such as micro- and capillary liquid chromatography (LC) [1]. Capillary electrophoresis (CE) also attracts much attention, especially because of its high separation efficiency for ionogenic analytes [2]. Unfortunately, such microseparation systems have the drawback that favourable concentration limits of detection (LODs) cannot easily be achieved. Detection volumes that can be tolerated without deteriorating the high separation efficiency, are no more than a few nanolitres. Lasers are therefore the most suitable light sources to perform spectrometric detection. Because of their high directionality, they allow efficient irradiation of small detection volumes.

Laser-induced fluorescence (LIF), the optical laser

*Corresponding author.

0021-9673/98/$19.00
PII: S0021-9673(98)00258-1

detection method most frequently used in combination with microseparation systems, provides favourable concentration LODs [3], but can only be applied directly to analytes exhibiting native fluorescence. There is therefore an obvious need for a laser-based detection method which has a wide applicability range as holds for absorption detection. In earlier research, it has been suggested that forward degenerate four-wave mixing (F-D4WM) can become such a technique. Like fluorescence spectroscopy, F-D4WM is a zero-background method, a special mode of thermal grating spectroscopy [4], which has been shown to provide good sensitivity if efficient background suppression can be achieved [5–11].

In the development of F-D4WM as an analytical tool, Tong and coworkers have played an important role [5–9]. Recently, they explored the applicability of F-D4WM detection in CE and showed interesting results [12]. In their study labelling of analytes with a chromophoric group (dabsyl chloride) had to be used to meet the requirement of laser light absorption in the visible range (457.8 nm); furthermore, the high molar absorptivity of the dabsyl group ($3 \cdot 10^4$ M^{-1} cm^{-1}) is not typical for analyte absorptivities in general. In our view, the F-D4WM technique will only have perspective as a detection technique in CE and micro-LC if derivatization can be avoided. If derivatization has to be used for reasons of detectability, the method of choice will be fluorescence labelling, preferably in the near-infrared region so that diode lasers can be used [13–15].

It is our intention to optimize F-D4WM detection by improving signal-to-background ratios by applying an appropriately detection cell assembly and by making use of an interferometer to discriminate between the coherent F-D4WM signal and the non-coherent background. To test the performance of the F-D4WM technique coupled to a micro-separation system, the detectability of two model compounds that absorb light in the visible region (though with less favourable absorptivities than the dabsyl group) after a micro-separation is studied. Secondly, we will study the ultraviolet region in order to achieve the wide-ranging applicability inherently provided by F-D4WM [10,11].

Despite the 'zero-background' character of F-D4WM, background reduction is of primary importance to achieve favourable LODs. Contrary to LIF detection, impurity fluorescence and Raman scatter do not contribute since F-D4WM detection is exclusively performed at the laser wavelength applied. The background in F-D4WM detection comes from scattering from the optical components (beam splitter, mirrors and lenses), the major contribution being scattering from the cell windows combined with internal reflections. Reduction of scatter has been achieved by using well-polished quartz windows of high optical quality. Internal reflections have been minimized by applying Brewster's angle at all four cell boundaries (i.e. two air–quartz boundaries and two quartz–liquid boundaries) [10]. Further background suppression has been achieved by means of a mechanical chopper in combination with a lock-in amplifier (LIA), a light polarization discrimination scheme and a scanning confocal Fabry–Perot interferometer in combination with a ramp generator and LIA. By applying the Brewster cell set-up in combination with a scanning interferometer, we have been able to detect an injected concentration of $2 \cdot 10^{-8}$ M of 1-amino-9,10-anthraquinone (molar absorptivity $2 \cdot 10^3$ M^{-1} cm^{-1} at the applied laser line) after a conventional-size LC separation [11]. It was noted that, despite the rather large dimensions of the detector cell, the irradiated volume is as small as 1 nl. This suggests that similar results can be achieved in miniaturized systems. To test this hypothesis, in the present paper F-D4WM detection is coupled to micro-LC, using a column with an internal diameter of 0.3 mm.

2. Theory

Forward-scattering four-wave mixing refers to the process where two forward-propagating laser beams, E_1 and E_2, interact in a medium and generate two signal beams, E_3 and E_4, spatially distinguishable from E_1 and E_2 [7,16,17]. When E_1 and E_2 intersect, an interference pattern is produced. If light is absorbed by the molecules at the ventral regions of the interference pattern, subsequent vibrational relaxation takes place and a thermally induced refractive index modulation with the same profile as the interference pattern will be generated. This refractive index modulation acts as a diffraction grating: diffraction of E_1 and E_2 leads to the formation of the

signal beams E_3 and E_4. These signal beams can be observed on a (theoretically) dark background: in the absence of absorbing molecules, no thermal grating is formed and diffraction cannot take place.

The intensities of the signal beams E_3 and E_4 are given by [7,18]:

$$I_3 = CI_1^2 I_2 \cdot \frac{\lambda_{ex}^2}{\sin^2\theta} \cdot \left[\frac{\partial n}{\partial T}\right]^2 \cdot m^2 \cdot \frac{\alpha^2 \eta^2}{\kappa^2} \quad (1)$$

$$I_4 = CI_1 I_2^2 \cdot \frac{\lambda_{ex}^2}{\sin^2\theta} \cdot \left[\frac{\partial n}{\partial T}\right]^2 \cdot m^2 \cdot \frac{\alpha^2 \eta^2}{\kappa^2} \quad (2)$$

In Eqs. (1) and (2), C is a constant; I_1 and I_2 are the excitation beam powers in W; λ_{ex} is the laser wavelength in nm, $\partial n/\partial T$ the temperature gradient of the refractive index in K^{-1}, α the absorptivity in cm^{-1} which is of course proportional to the analyte concentration, θ the angle between the excitation beams, κ the thermal conductivity of the solvent in mW cm^{-1} K^{-1}, m a 'mixing quality' parameter (depending on parameters such as overlap of the excitation beams, optical pathlength in the detector cell, coherence length of the laser and the quality of the cell windows), which varies between 0 and 1. Finally, η is the efficiency of conversion of photon energy into heat for an analyte, which contributes to the thermal grating and can be expressed as:

$$\eta = 1 - \phi_L \quad (3)$$

where ϕ_L is the luminescence quantum yield. Obviously, for a non-fluorescent molecule ($\phi_L = 0$), Eq. (3) is fully adequate; in this case η is 100% and all the excitation energy is completely converted into heat. However, for a molecule with 100% luminescence quantum yield, η is not equal to zero. This will be immediately obvious from Fig. 1, which shows the photophysical processes for the two examples concerned. Also for a molecule with ϕ_L equal to 100%, upon excitation heat is produced, caused by vibrational relaxation both in the electronic excited state and in the electronic ground state. Therefore, even for fluorescent compounds with 100% fluorescence quantum yield, heat is still dissipated to the surrounding solvent molecules which will contribute to the thermally induced refractive index grating. To account for this phenomenon, in a second approximation Eq. (3) should be rewritten as:

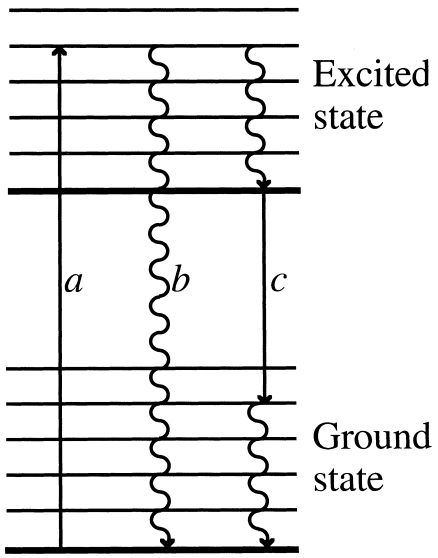

Fig. 1. Simple Jablonski diagram including the pathways of a molecule upon excitation: a = absorption; b = non-radiative decay; c = radiative decay. The wavy arrows indicate heat production due to vibrational relaxation, which will contribute to the thermal grating. The solid arrows indicate optical transitions.

$$\eta = 1 - \phi_L \cdot \frac{\lambda_{ex}}{\lambda_{em}} \quad (4)$$

where λ_{em} is the emission wavelength. However, since fluorescence emission is broad-banded (in liquids), in a final approximation one has to average the ratio $\lambda_{ex}/\lambda_{em}$ over the emission band. Therefore, Eq. (4) should ultimately be written as:

$$\eta = 1 - \phi_L \cdot \frac{\int_{\lambda_{ex}}^{\infty} \frac{\lambda_{ex}}{\lambda} I_L(\lambda) d\lambda}{\int_{\lambda_{ex}}^{\infty} I_L(\lambda) d\lambda} \quad (5)$$

where $I_L(\lambda)$ is the luminescence intensity as a function of the emission wavelength and the denominator is introduced to normalize $I_L(\lambda)$. The lower limit of integration is taken as λ_{ex}, since no luminescence can be expected at wavelengths shorter than the excitation wavelength.

In Table 1, Eqs. (3)–(5) are evaluated for some typical examples, covering fluorescence quantum yields from 0.01% up to about 100%. For the three unsubstituted polynuclear aromatic hydrocarbons

Table 1
Evaluation of η according to Eqs. (3)–(5) for some typical polyaromatic compounds

Compound	ϕ_L	η according to equation:		
		3	4	5
Perylene*	0.94[a]	0.06	0.31	0.32
Anthracene*	0.36[a]	0.64	0.69	0.70
Pyrene*	0.32[a]	0.68	0.73	0.72
I-AAQ	0.01[b]	0.99	0.99	0.99
II-AAQ	$1 \cdot 10^{-4}$[b]	1.00	1.00	1.00

For the three polynuclear hydrocarbons denoted by an asterisk, λ_{ex} was set equal to 340 nm. For the aminoanthraqunones, a wavelength of 514 nm is taken for λ_{ex}, in conformity with the present experiments.
[a]From Ref. [22].
[b]From Ref. [23].

involved, λ_{ex} was set equal to 340 nm, an excitation wavelength frequently used in practice. Table 1 shows that the further refinement given by Eq. (5) does hardly lead to improvement. On the other hand, the correction term introduced in Eq. (4) is of distinct importance, especially for fluorophores with quantum yields higher than 50%, as is demonstrated for perylene. In fact, the range in η values in Table 1 is only from 30 to 100%, in marked contrast with the associated ϕ_L values which vary over four decades. This phenomenon is further illustrated in Fig. 2 which shows a plot of η versus ϕ_L for a typical $\lambda_{ex}/\lambda_{em}$ ratio of 0.8: even for $\phi_L = 1.00$, η is as large as 20%. The above considerations lead to the conclusion that, in principle, F-D4WM detection is as widely applicable as UV–Vis absorption detection; maybe rather unexpectedly, it can also be used for strongly fluorescent compounds (though with reduced efficiency).

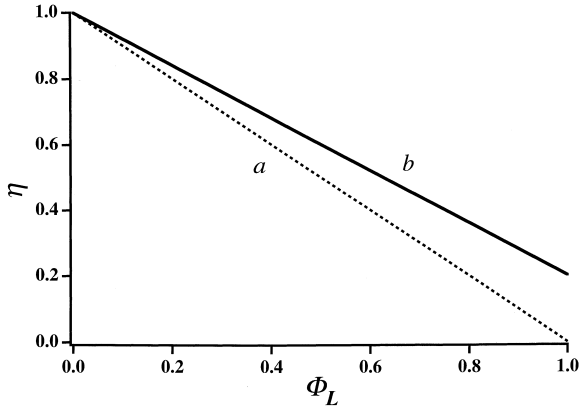

Fig. 2. Calculated plot of η versus ϕ_L, (a) ignoring the difference between λ_{ex} and λ_{em} (dotted curve) and (b) assuming $\lambda_{ex}/\lambda_{em} = 0.8$ (solid curve).

A characteristic feature of the F-D4WM signal is its coherency. As will be outlined below, this feature can be used to improve the signal-to-background, and thus the signal-to-noise ratio achievable. As noted above, background radiation has the same wavelength as the signal: It is caused by scatter and reflection at the air-to-quartz and quartz-to-liquid boundaries (although it is strongly reduced by utilizing Brewster's angle) and, presumably, its coherence is largely lost. This difference in coherence allows to discriminate the coherent signal from the non-coherent scattered light by means of a confocal Fabry–Perot interferometer (CFP) [11]. The characteristic features of the CFP are well documented in the literature [11,19]. In the Appendix, the equations describing its transmission, which are schematically shown in Fig. 7, are presented. It will be calculated that, for the mirrors applied in our CFP, the discrimination factor between coherent and non-coherent light will be 2500. Therefore, the concentration LOD, which under shot-noise conditions is related to the square root of the signal, is theoretically expected to be 50-fold improved by using the CFP compared to a set-up without background reduction.

3. Experimental

3.1. LC separation

The micro-LC system consisted of an LC pump (LKB, Model 2150, Pharmacia, Sweden), a laboratory-made pulse dampener, a T-piece based flow splitter, an injection valve (Valco, Schenkon, Switzerland) and a 25·0.3 mm capillary column packed with 5 μm C_{18}-bonded silica (LC Packings, Amsterdam, The Netherlands). A T-piece was used to split the flow of 0.25 ml min^{-1} into a flow back to the eluent reservoir (via a restriction capillary, I.D. 20 μm, length 20 cm) and a flow of 4 μl min^{-1} to the injection valve. The micro-injection valve was used to inject 600 nl of sample on the micro-column. The analytes were separated by isocratic elution

using methanol–phosphate buffer (90:10, v/v) as the eluent. They were dissolved in methanol–phosphate buffer (75:25, v/v) to achieve 'on-column focusing' [20]. The outlet capillary of the column was connected to the UV–Vis absorption detector, or to the flow cell of the F-D4WM set-up, which will be described below. All connecting capillaries (I.D. 50 μm; O.D. 280 μm) were kept as short as possible; the connections were made by low-pressure PTFE tubing (LC Packings, catalogue code TF250).

3.2. Chemicals

1-Amino-9,10-anthraquinone (I-AAQ) and 2-amino-9,10-anthraquinone (II-AAQ) were purchased from Fluka (Buchs, Switzerland) and used as received. Methanol ('Baker grade') was obtained from Baker (Deventer, The Netherlands). The buffer was an aqueous 10 m*M* solution of phosphoric acid (Baker) adjusted to pH 6.9 with concentrated NaOH solution. NaOH was obtained from Riedel–De Haën (Seelze, Germany).

3.3. Absorption detection

A conventional LC absorption detector (Kratos, Ramsey, NJ, Model Spectroflow 757) was used; its cell was replaced by a U-shaped capillary flow cell (LC Packings, catalogue code UZ-AB-CAP) with an optical path length of 8 mm and an I.D. of 75 μm. In order to compare the results with the F-D4WM set-up, the absorbance was recorded at 514 nm. The time constant was set to 1.0 s. The output was digitized by a home-made A/D converter (16 bits resolution, 10 Hz acquisition rate) and sent to an Apple Macintosh LC computer for further analysis.

3.4. Laser

A large-frame argon-ion laser (Coherent, Model Innova 100, Palo Alto, CA, USA) was used, which delivered 800 mW of optical power at 514.5 nm. By inserting an intracavity etalon (Coherent, Model 924), single-frequency operation was established: the lasing bandwidth was narrowed from 6 GHz (0.2 cm^{-1}) to 150 MHz (0.05 cm^{-1}), which implies an increase of coherence length from 5 cm to 2 m.

3.5. F-D4WM set-up

The laser beam passes a holographic bandpass filter for 514 nm (Kaiser Optical Systems, Ann Arbor, MI, USA) in order to reject spontaneous radiation and non-lasing emission lines from the discharge in the plasma tube of the argon ion laser. The beam is subsequently split by a variable polarizing beam splitter (CVI, Albuquerque, NM, USA) to realize the optimum splitting ratio of 2:1 (I_1:I_2). A $\lambda/2$ retardation plate (CVI) was applied to restore beam E_2 to its (original) vertical polarization. The beams are made parallel and then focused and mixed simultaneously in the flow cell by means of a 100-mm focal-length lens (CVI). After mixing in the flow cell, the pump beams E_1 and E_2 and the weaker signal beam E_4 are blocked; the signal beam E_3 is collected by a 100-mm focal-length lens. Next, the beam is filtered by a spatial filter (Spectra Physics, Palo Alto, CA, USA; Model 332; pinhole 22 μm) and the scanning Fabry–Perot interferometer. The CFP was removed during the experiments with the mechanical chopper. An interference filter for transmission at 514 nm is used to reject any fluorescence or Raman light. Finally, the beam is detected by a photomultiplier tube (Philips, Eindhoven, The Netherlands, Model XP2020Q) operated at 1600 V. During the experiments with the mechanical chopper, the chopper (EG&G, Princeton, NJ, USA, Model P/N 651-1) was placed in the E_2 pathway of the set-up. The lock-in amplifier (Princeton Applied Research, Princeton, NJ, USA, Model HR-8) was set at 495 Hz (during the experiments with the chopper) or 990 Hz (during the experiments with the scanning interferometer). The output of the photomultiplier was digitized by the laboratory-made A/D converter (see Section 4.1) and sent to the Apple Macintosh computer.

3.6. Cell design

To interface the F-D4WM technique to micro-LC, a Brewster cell was designed as shown in Fig. 3 [10]. The cell consists of two wedged (wedge angle 7°, which is the difference in angle between Brewster's angle for the air-to-quartz and the liquid-to-glass transition) Suprasil I quartz windows separated by a PTFE spacer of thickness 0.8 mm tightened by two

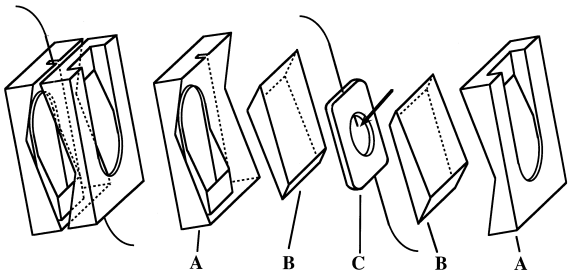

Fig. 3. Left-hand side: schematic drawing of the Brewster flow cell; right-hand side: Brewster flow cell assembly. A = PEEK clamps; B = Suprasil I quartz windows, wedge angle 7°; C = PTFE spacer pierced by fused-silica capillaries. The laser beams should be positioned as indicated by the arrow.

polyether ether ketone (PEEK) clamps. The cell volume was 5 μl, which is obviously too large for micro-LC. However, by directing the focused laser beams just below the outlet capillary of the column, the effect of band broadening can be reduced. The width of the chromatographic peak was compared to that of the injected plug to estimate the dilution caused by the detection technique.

3.7. Interferometer

Details of the scanning CFP have been reported in an earlier paper [11]. The home-made device consists of two partly transmitting mirrors (CVI, radius of curvature: 5 cm, reflection R: 0.98 and separation distance d: 5 cm), one being mounted on a piezo electrical element connected to a home-made ramp generator to alternate the mirror spacing. A value R of 0.98 was a good compromise between the theoretically attainable discrimination factor between coherent/incoherent radiation and the ease of alignment (which is more critical when R approaches 1.0). The housing of the interferometer was made of Nilo, a material with a low coefficient of thermal expansion. The scanning voltage, provided by a home-made ramp generator, had a frequency of 990 Hz and the ramp wave form was triangle-shaped. The periodic displacement of the mirror mounted on the piezo element was 125 nm ($\approx\lambda/4$), which is enough to achieve complete constructive and destructive interference, so that maximum amplitude modulation of the (coherent) signal could be achieved.

4. Results and discussion

4.1. Conventional absorption detection

A chromatogram of the I-AAQ/II-AAQ mixture obtained with the micro-LC system using absorption detection by means of the U-shaped capillary flow cell is depicted in Fig. 4. From this chromatogram, an injected concentration LOD of $5\cdot10^{-6}$ M can be calculated for I-AAQ and $1\cdot10^{-5}$ M for II-AAQ (S/N is 3, where N is the peak-to-peak noise). The

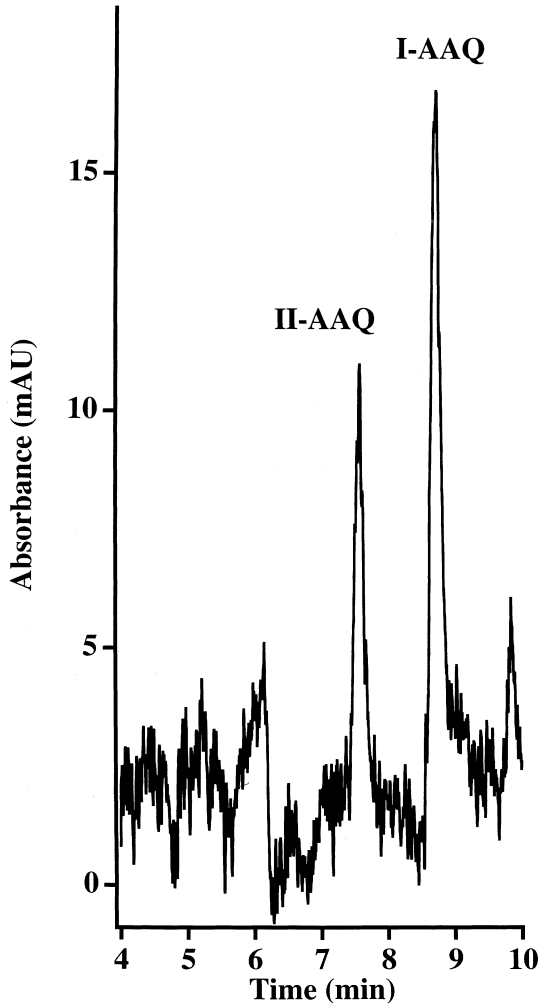

Fig. 4. Micro-LC chromatogram of a mixture of two isomers of amino-9,10-anthraquinone obtained by absorbance detection at 514 nm. Injected concentrations: $1\cdot10^{-5}$ M for I-AAQ and $2\cdot10^{-5}$ M for II-AAQ.

dilution due to the chromatographic process, which can be calculated from the chromatogram, is only a factor 1.2, which indicates the good quality of the separation system. Nonetheless, compared to absorption detection in conventional-size LC, the above mentioned LODs imply a decrease in sensitivity by about two decades, despite the fact that the optical pathlengths in a standard LC flow cell and the U-type absorption detection cell in micro-LC are the same (8 mm). This loss can primarily be attributed to the considerable reduction in cross-sectional area (1.3 mm^2 compared to 0.002 mm^2), which strongly hinders the light throughput and, for a minor part, to the shorter response time used in micro-LC (1.0 s compared to 3.0 s in conventional-size LC) [21].

4.2. F-D4WM measurements

Two strategies were used to perform F-D4WM detection. In order to minimize the effect of background radiation due to scattered and reflected pump beams, a lock-in detection scheme with a mechanical chopper combined with a lock-in amplifier was used. The chromatogram thus obtained is shown in Fig. 5. The injected concentration LOD calculated from this chromatogram is only slightly (2- to 3-fold) better than the values reported above: $2 \cdot 10^{-6}$ *M* for I-AAQ and $4 \cdot 10^{-6}$ *M* for II-AAQ. The situation is even worse when peak shapes are considered as well. Increased band broadening and peak tailing are observed, which are most probably caused by the turbulence of the liquid stream close to the outlet capillary entering the large volume of the flow cell. A dilution factor of 2.3 can be calculated from the chromatogram, indicating serious loss of resolution. An attempt to diminish these effects by positioning the waist of the laser beam close to the capillary outlet unfortunately resulted in a higher background: part of the beam is scattered on the tip of the capillary and this scattered light propagates in the same direction as the F-D4WM signal beam. The laser beam is at optimum position when no scatter from the tip of the capillary is observed. The conclusion is that, in view of these results and concerning the complexity of the technique, F-D4WM detection in combination with mechanical chopping shows little perspective and will never replace conventional absorption detection.

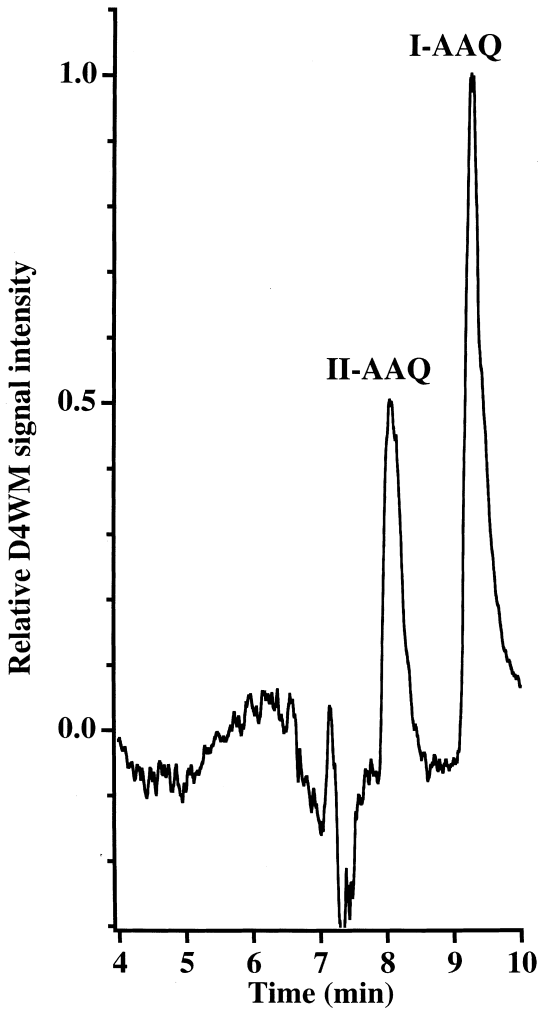

Fig. 5. Micro-LC chromatogram of a mixture of I-AAQ and II-AAQ utilizing F-D4WM detection at 514 nm with the mechanical chopper/LIA combination. Injected concentrations: $4 \cdot 10^{-6}$ *M* for I-AAQ and $8 \cdot 10^{-6}$ *M* for II-AAQ.

Improved detection limits in F-D4WM can be expected if interferometric discrimination of signal and background is introduced. A typical chromatogram is shown in Fig. 6 for injected concentrations of $5 \cdot 10^{-8}$ *M* I-AAQ and $1 \cdot 10^{-7}$ *M* II-AAQ. These correspond with LODs of $3 \cdot 10^{-8}$ *M* for I-AAQ and $5 \cdot 10^{-8}$ *M* for II-AAQ, which can be even further improved three-fold by enhancing the laser power to 1.2 W. Apparently, considerable improvement in detectability of F-D4WM compared with absorption detection can be achieved due to the signal-to-back-

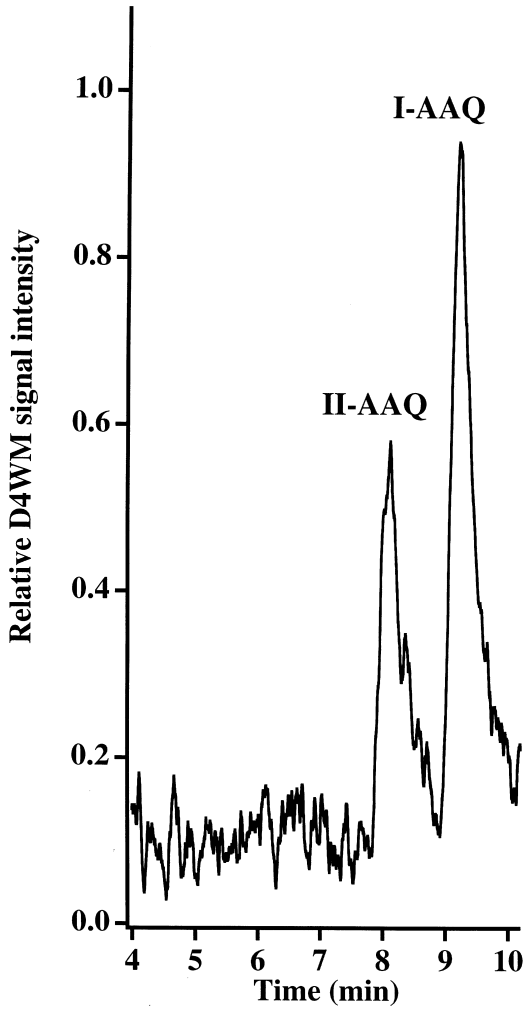

Fig. 6. Micro-LC chromatogram of a mixture of I-AAQ and II-AAQ utilizing F-D4WM detection at 514 nm with the interferometer/LIA combination. Injected concentrations: $5 \cdot 10^{-8}$ *M* for I-AAQ and $1 \cdot 10^{-7}$ *M* for II-AAQ.

ground discrimination performed by the scanning interferometer. Comparison of the chromatograms depicted in Figs. 4 and 6 reveals that also in this F-D4WM set-up strong band broadening takes place (dilution factor calculated as large as 5.4). Apparently, the illuminated volume is not close enough to the outlet of the capillary and further modifications of the detection cell are required to guarantee the chromatographic integrity. Thus far, LODs associated with injected analyte concentrations were considered. Of course, under serious band broadening conditions, the corresponding concentrations in the detection cell are much lower. This holds especially for Fig. 6; if the dilution factor of 5.4 is taken into account, the lowest concentrations in the detector that can be measured are $6 \cdot 10^{-9}$ *M* for I-AAQ and $9 \cdot 10^{-9}$ *M* for II-AAQ (at 800 mW laser power). Compared with the F-D4WM set-up using a mechanical chopper, the gain in analyte detectability is two decades, which is in good agreement with the calculated factor of 50 (see Theory section and Appendix).

To evaluate the significance of the present results, some F-D4WM data on concentration LODs for I-AAQ are collected in Table 2, while for convenience also the micro-LC data using absorption detection are included. Both injected and detected concentrations are shown, the latter being based on the dilution factors calculated from the chromatograms considered. Table 2 reveals some interesting features. (i) F-D4WM detection is only of interest if combined with the scanning confocal interferometer. (ii) Upon miniaturization from conventional-size to micro-LC in the F-D4WM detection mode (combined with CFP) there is essentially no loss in

Table 2
F-D4WM and absorption detection of I-AAQ at 514 nm in micro-LC and conventional-size LC when applying a mechanical chopper or a scanning CFP

Separation method	Detection method	Background reduction	Laser power (mW)	Conc. LOD injected (*M*)	Conc. LOD detected (*M*)[a]	Ref.
Conv. size LC	F-D4WM	chopper	500	$6 \cdot 10^{-7}$	$1 \cdot 10^{-7}$	[9]
Conv. size LC	F-D4WM	CFP	500	$2 \cdot 10^{-8}$	$3 \cdot 10^{-4}$	[10]
Micro-LC	F-D4WM	chopper	800	$2 \cdot 10^{-6}$	$9 \cdot 10^{-7}$	This work
Micro-LC	F-D4WM	CFP	800	$3 \cdot 10^{-8}$	$6 \cdot 10^{-9}$	This work
Micro LC	absorption	–	–	$5 \cdot 10^{-6}$	$4 \cdot 10^{-6}$	This work

[a]For the detected concentration LODs listed, the dilution of the injected plug due to band broadening (calculated from the observed peak widths) was taken into account.

detectability in concentration units. This is in marked contrast with conventional absorption detection where such a miniaturization implies serious reduction of analyte detectability, as illustrated by the above results, and in line with the literature [21]. (iii) In micro-LC the concentration LODs observed using F-D4WM (with CFP) detection are two orders of magnitude more favourable than for absorption detection, i.e. of $3\cdot10^{-8}$ *M* and of $5\cdot10^{-6}$ *M*, respectively. In view of the corresponding calculated concentrations in the detector cell (of $6\cdot10^{-9}$ *M* and of $4\cdot10^{-6}$ *M*, respectively), this difference can, in principle, be further enhanced to three decades, provided that it is possible to construct a F-D4WM detection cell that does not contribute to band broadening.

Finally, it is tempting to compare the data in Table 2 with the results on dabsyl-derivatized amino acids separated by CE, recently published by Wu and Tong [12]. They reported an injected concentration LOD of $1.8\cdot10^{-6}$ *M* for dabsyl-glycine (and a calculated concentration LOD in the detector cell of $9\cdot10^{-8}$ *M*; based on a dilution factor as high as 20). Unfortunately, there are too many parameters involved to make such a comparison meaningful. For example, Wu and Tong straightforwardly used the CE capillary for detection instead of a Brewster-angle-based detection cell and, thus, had to deal with intense background scatter. Furthermore, they applied a wavelength of 458 nm at a power level of 30 mW (instead of 514 nm laser light at 0.8 W) and monitored the dabsyl chromophore with a molar absorptivity of $3\cdot10^{4}$ $M^{-1}\text{cm}^{-1}$ (at 458 nm), instead of I-AAQ with a molar absorptivity of $2\cdot10^{3}$ $M^{-1}\text{cm}^{-1}$ (at 514 nm). A quantitative comparison will be made in a forthcoming paper in which a capillary will be used for detection, to avoid band broadening at the cost of a higher background.

5. Conclusions

The present results unambiguously show the feasibility of the F-D4WM technique for detection in miniaturized systems such as micro-LC. The improvement in injected concentration detection limits compared to absorption detection (for the model compound I-AAQ) from $5\cdot10^{-6}$ *M* to $3\cdot10^{-8}$ *M* is quite significant. This result is mainly caused by the use of a scanning confocal Fabry–Perot interferometer for background suppression.

Unfortunately, the performance of the detector cell is still far from ideal. The laser beam cannot be positioned close enough to the capillary outlet to prevent unwanted band broadening. Therefore, modification of the detector cell is required; in fact it will be a challenge to construct a similarly designed Brewster cell with dimensions compatible with micro-LC. Next, the F-D4WM detection technique will have to move from the present 514 nm towards the ultraviolet region to extend its application range.

Acknowledgements

This research was funded by the Dutch Foundation for the Advancement of Science (NWO) and Chemical Research (SON) under grant number 700-44-006.

Appendix 1

Performance of the scanning confocal Fabry–Perot interferometer

A schematic presentation of the Fabry–Perot interferometer principle is given in Fig. 7.

A confocal Fabry–Perot interferometer (CFP) basically consists of two identical partially transmitting mirrors (with reflection $R=r^2$ and transmission $T=t^2=1-R$) separated by a distance *d* [19]:

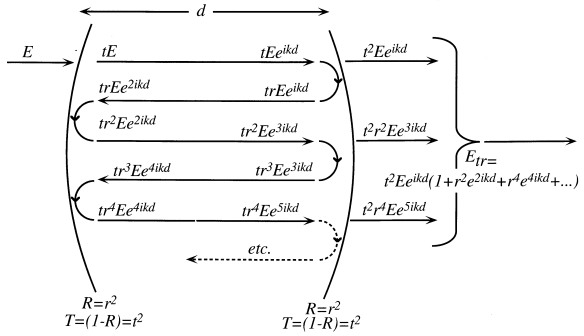

Fig. 7. Schematic presentation of the Fabry–Perot interferometer principle.

A coherent incident wave, E, which passes the CFP results in a transmitted wave, E_{tr}:

$$E_{tr} = t^2 e^{ikd} E + t^2 r^2 e^{3ikd} E + t^2 r^4 e^{5ikd} E + \cdots$$
$$= t^2 e^{ikd} E(1 + r^2 e^{2ikd} + r^4 e^{4ikd} + \cdots) \quad (6)$$

The factor e^{ikd} accounts for the change of phase of the wave on going from the entrance to the exit of the CFP. By applying geometric progression:

$$1 + x + x^2 + x^3 + \cdots = \frac{1}{(1-x)} \quad (-1 < x < 1) \quad (7)$$

one can rewrite Eq. (6) as:

$$E_{tr} = \frac{t^2 e^{ikd} \cdot E}{1 - r^2 e^{2ikd}} \quad (8)$$

The transmittance of the CFP, denoted as T_{CFP}, is:

$$T_{CFP} = \frac{E_{tr} E_{tr}^*}{E E^*} = \frac{t^4}{1 + r^4 - 2r^2 \cos(2kd)}$$
$$= \frac{T^2}{1 + R^2 - 2r^2 \cos(2kd)}$$
$$= \frac{(1-R)^2}{(1-R)^2 + 4R \sin^2(kd)} \quad (9)$$

where E^* and E_{tr}^* are the complex conjugates of E and E_{tr}, respectively. For a coherent beam, T_{CFP} is equal to 1 if kd is a multiple of π. In this case, constructive interference takes place. Since $k = 2\pi/\lambda$, the requirement for d is:

$$d = m \cdot \frac{\lambda}{2} \quad (m \text{ is any integer}) \quad (10)$$

When d is made equal to $(m + 1/2)\lambda/2$, destructive interference will take place and the transmission of the CFP will drop to:

$$T_{CFP,DI} = \frac{(1-R)^2}{(1-R)^2 + 4R} \quad (11)$$

where the additional subscript DI stands for destructive interference. The waves of a non-coherent beam have no phase relation with each other, and therefore no constructive or destructive interference takes place. In that case, each mirror of the CFP acts as an attenuator with an transmittance $(1-R)$ which will result in an overall transmittance of the CFP for non-coherent light of $(1-R)^2$. For the mirrors applied in this study $R = 0.98$; therefore, the discrimination factor between coherent and non-coherent radiation is 2500, so that under shot-noise conditions the concentration LOD will be 50-fold improved.

The discrimination factor can be further enhanced by alternating the mirror separation distance, d, by means of a piezo-electrical element. This makes the CFP alternatingly fully transparent and totally reflective for coherent light; hence, the coherent signal will be amplitude-modulated synchronously with the scanning voltage applied to the piezo element. For non-coherent light, the transmittance of the CFP does not depend on the mirror separation d so that no modulation takes place. When using phase-sensitive detection of the transmitted light by means of a lock-in amplifier, the small DC component originating from the non-coherent background will be completely suppressed, which may result in further enhancement of the signal-to-background ratio. The data in Table 2 indeed indicate that there is an effect of scanning. The LODs in the detector cell obtained in the chopper mode and the CFP mode are $9 \cdot 10^{-7}$ M and of $6 \cdot 10^{-9}$ M, respectively, reflecting a 150-fold improvement, three times higher than calculated for the static CFP mode.

References

[1] J.P. Chervet, M. Ursem, Anal. Chem. 68 (1996) 1507.
[2] M. Ng, T.F. Blasche, A.A. Arias, R.N. Zare, Anal. Chem. 64 (1992) 1982.
[3] W.G. Kuhr, E.S. Yeung, Anal. Chem. 60 (1988) 2642.
[4] M.J. Pelletier, J.M. Harris, Anal. Chem. 55 (1983) 1537.
[5] Z. Wu, W.G. Tong, Anal. Chem. 61 (1989) 998.
[6] Z. Wu, W.G. Tong, Anal. Chem. 63 (1991) 1943.
[7] Z. Wu, W.G. Tong, Anal. Chem. 65 (1993) 112.
[8] S. Berniolles, Z. Wu, W.G. Tong, Spectrochim. Acta 49B (1994) 1473.
[9] Z. Wu, J. Liu, W.G. Tong, Spectrochim. Acta 49B (1994) 1483.
[10] T. de Beer, G.Ph. Hoornweg, G.J. Grootendorst, N.H. Velthorst, C. Gooijer, Anal. Chim. Acta 330 (1996) 189.
[11] G.Ph. Hoornweg, T. de Beer, N.H. Velthorst, C. Gooijer, Appl. Spec. 51 (1997) 1008.
[12] Z. Wu, W.G. Tong, J. Chromatogr. A 773 (1997) 291.
[13] A.J.G. Mank, H.T.C. van der Laan, H. Lingeman, C. Gooijer, U.A.Th. Brinkman, N.H. Velthorst, Anal. Chem. 67 (1995) 1742.

[14] A.J.G. Mank, E.S. Yeung, J. Chromatogr. A 708 (1995) 30.
[15] A.J.G. Mank, M.C. Beekman, N.H. Velthorst, U.A.Th. Brinkman, H. Lingeman, C. Gooijer, Anal. Chem. 67 (1995) 1742.
[16] R.A. Fisher (Ed.), Optical Phase Conjugation, Academic Press, New York, 1983.
[17] C.V. Heer, N.C. Griffen, Opt. Lett. 4 (1979) 239.
[18] F. Simoni, G. Cipparone, D. Duca, I.C. Khoo, Opt. Lett. 16 (1991) 360.
[19] A. Yariv, Optical Electronics, CBS College Publishing, New York, 1985, Chap. 4.
[20] B.L. Ling, W. Baeyens, J. Microcol. Sep. 4 (1992) 17.
[21] E.S. Yeung, in: P.R. Brown, E. Grushkea (Eds.), Advances in Chromatography, Vol. 35, Marcel Dekker, New York, NY, 1995, Ch. 1.
[22] I.B. Berlman, Handbook of Fluorescence Spectra of Aromatic Molecules, Academic Press, New York, 1965.
[23] H. Inoue, M. Hida, N. Nakashima, K. Yoshihara, J. Phys. Chem. 86 (1982) 3184.